

Rain Attenuation on Short Radio Paths: Theory, Experiment, and Design

By W. F. BODTMANN and C. L. RUTHROFF

(Manuscript received January 9, 1974)

The outage time on short radio paths at frequencies above 10 GHz can be estimated from distributions of point rain rates derived from U. S. Weather Service rain gauge charts. In this paper, a previous theory is extended to include the effects of path length and frequency. Experimental corroboration is presented for three locations on the east coast of the United States, and the design of short radio paths is illustrated by examples. One-minute rain rate distributions for 20 locations are also included.

I. INTRODUCTION

Many characteristics of radio systems above 10 GHz are due to the existence of large attenuation by rain. These characteristics have been discussed at length in a previous publication.¹ The economical design of a system operating at these frequencies requires a knowledge of the incidence of rain attenuation at the location of the system; to be more specific, it requires a procedure for predicting the number of minutes per year that a radio path will be out of service because of excessive rain attenuation. This paper describes such a design procedure and includes data required to design systems in several sections of the country; design examples are also given.

The starting point for this design procedure is the theory of attenuation by uniform rainfall² and a relationship, derived in Ref. 3, between the attenuation distribution measured on a path and a point rain rate distribution measured near the path. The key result of Ref. 3 is a connection between the theory of attenuation of uniform rain and that of the variable rainfall experienced in practical situations. This connection is, of course, vital to any practical measurement because uniform rain does not usually occur. A conclusion of this work was that the measuring interval used in rain rate measurements has a large

effect on the accuracy of the predicted attenuation distribution. A definition of rain rate suited to the prediction of attenuation distributions was provided, and it was shown that, if the rain rate distribution were measured in the proper way, the attenuation distribution could indeed be estimated from it.

The importance and usefulness of the theoretical result lies in the existence of point rain rate data from a large number of rain gauges all over the country.⁴ Copies of charts from many of these recording gauges can be obtained from the U. S. Weather Service.* However, these charts do not record rain rates directly, and initially it was far from obvious that appropriate rain rate data could be obtained from them at all. Thus, the transformation from an interesting theory to practical engineering application came when a method was devised for measuring accurate 1-minute rain rate distributions from these rain gauge charts.

This paper begins with a brief review of the salient results in Ref. 3, and extends that theory to include the effects of frequency and path length. Since a theory of design is only as good as its results, predictions of attenuation distributions computed from rain rate distributions are compared with attenuation distributions measured on several paths, and in all cases the agreement is excellent. The paper concludes with examples of the design of short radio paths in several sections of the country.

II. REVIEW OF THEORY³

A theory of attenuation of uniform rainfall has been formulated by Ryde and Ryde and others, and a good account is given by Medhurst.⁵ The attenuation resulting from uniform rain has been computed by Ryde and Ryde,² Medhurst,⁵ and Setzer;⁶ Setzer's results, for several frequencies of interest, are shown in Fig. 1.

Any relationship between attenuation and rain rate must take into account the fact that attenuation depends upon the density of rain in the path and is therefore a volume function, whereas rain rate is a surface vector, the magnitude of which is the rate of water flowing through a surface area.

For uniform rainfall, the relationship between rain rate and rain density on the path is simple and not at all dependent upon the time interval used in the rain rate measurement. However, uniform rainfall

* U. S. Department of Commerce, National Oceanic and Atmospheric Administration, Environmental Data Service, National Climatic Center, Federal Building, Asheville, N. C. 28801.

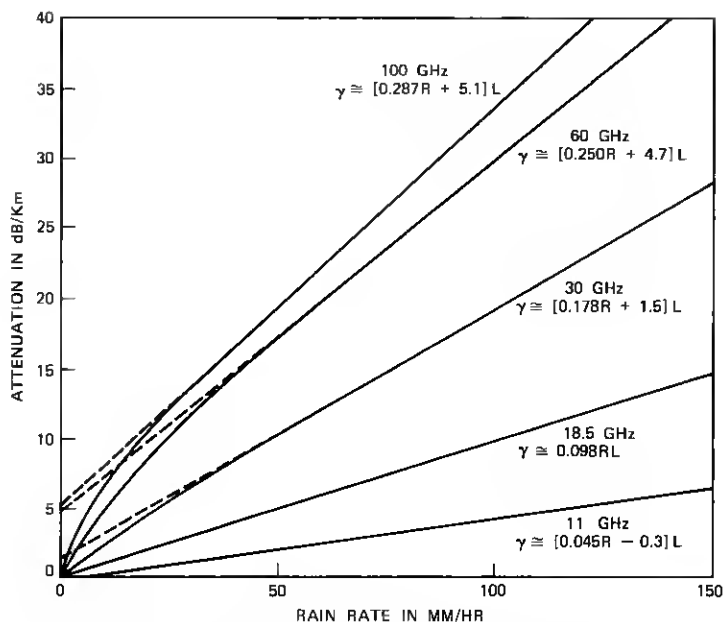


Fig. 1—Computed attenuation as a function of rain rate and frequency.

is not encountered in nature; both the density of rain on the path and the rain rate are functions of position and time. The divergence theorem can be used to relate the rain density, which is a volume function, to the rain rate, which is a surface vector. The volume chosen for the application of the divergence theorem to a radio path is shown in Fig. 2. It is the first Fresnel ellipsoid, a prolate ellipsoid with major axis L and minor axis $\sqrt{\lambda L}$. The path length is L and the wavelength of the transmission is λ . Typically, the ratio of these axes on short paths is on the order of 500. This volume is chosen because substantially all the power that reaches the receiver passes through it.

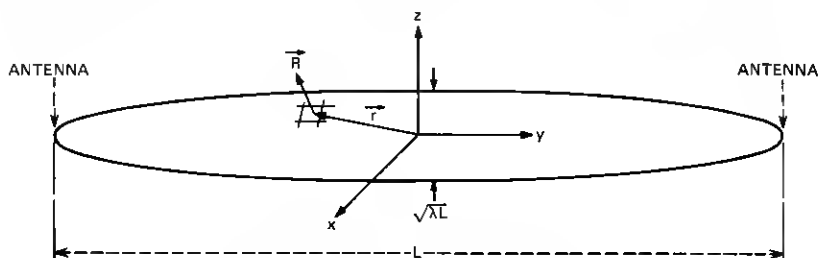


Fig. 2—An ellipsoidal surface enclosing the radio path.

If the rain rate is known at every point on the surface at all times, the volume of rain in the path can be computed.³ However, rain rate must be measured in a specified time interval—called integration time—and if the interval is too long, important fine structure in the rain rate—and the resulting fades—could be missed.

The path geometry can be used to determine an interval short enough so that no deep fades will be missed. The time required for a deep fade to develop is related to the time required for the rain to fill a large fraction of the volume of the ellipsoid in Fig. 2. For a step function of rain with velocity V , the minimum time for the volume to fill is $\sqrt{\lambda L}/V$. It follows that a deep fade will not occur in a time $T_0 \ll \sqrt{\lambda L}/V$. Thus, a rain gauge with an integration time T_0 should be sufficiently fast for our purpose. Actually, of course, step functions of rain do not occur, and an integration time T larger than T_0 will suffice. For a practical rain gauge design, T_0 serves only as a guide and as assurance that a suitable rain gauge is at least possible.

Since rain rate cannot be measured at all points on the surface of the path, it is necessary to consider what can be done with a single rain gauge in the vicinity of the path.

Fortunately, the attenuation as a function of time is not required; for radio path design, knowledge of the fraction of time that the path attenuation exceeds the fading margin is sufficient. To determine this information, we need to relate the point rain rate distribution to the path attenuation distribution. The method of relating these distributions is described in Ref. 3, and only pertinent results will be given here. If we measure the point rain rate distribution for a small enough integration time and are then able to obtain distributions for multiples of this interval, an estimate of the path attenuation distribution can be computed from the point rain rate distribution obtained for a suitable integration time T . The appropriate integration time T is a function of path length and frequency and is discussed in Section III. A rain gauge that measures rain rate as prescribed by the theory is described in Section IV.⁷

III. RAIN RATE INTEGRATION TIME AS A FUNCTION OF PATH LENGTH AND FREQUENCY

The theory has so far produced a rain rate integration time T_0 sufficiently short that no significant rates will be missed. It is, of course, expected to be unnecessarily short because it was derived for severe and unrealistic conditions. For a given path and wavelength, there is an integration time T for the point rain rate measurement for which

the point rain rate distribution best approximates the path average rain rate distribution. Thus, the attenuation distribution is related to frequency and path length through the rain rate integration time T . The rate at which the path average rain rate changes depends upon the dimensions of the path. We assume, therefore, that the integration time in seconds is proportional to the distance through the path of Fig. 2, averaged over all trajectories through the center.

$$T = \frac{1}{V_c} \frac{\sqrt{\lambda L}}{\pi} \ln 32 \frac{L}{\lambda}, \quad (1)$$

where

L is the path length in meters,

λ is the wavelength in meters, and

V_c is a constant with the dimension of velocity.

The constant V_c is determined experimentally from measured attenuation and point rain rate distributions. From data to be discussed later, $V_c \approx 0.95$ meter per second.

IV. THE FAST INTEGRATING RAIN GAUGE: RAIN RATE DISTRIBUTIONS AS A FUNCTION OF INTEGRATION TIME

A rain gauge designed to measure rain rates in accordance with the requirements of the theory is shown schematically in Fig. 3.⁷ Rain is collected in a funnel with a 16-inch diameter. The water is directed by the small rotating funnel to one of four glass tubes. The tube receives the rain collected in a 1.5-second interval, and then the small funnel rotates to the next tube. After the water has settled in the first tube, its volume is measured by measuring the capacitance between two metallic plates attached to the outer surface of the tube. After the measurement, the tube is emptied and is ready to be used again. In this manner, the rain rate is measured in successive intervals of 1.5 seconds. Since all intervals are measured, it is simple to obtain rain rates for intervals that are multiples of 1.5 seconds.

The effect of rain rate integration time is shown in Fig. 4, in which the data were taken from the fast rain gauge. As expected, the highest rain rates are recorded for the shortest integrating time. From Fig. 4, it is clear that the rain rate distributions depend upon the integration time.

Figure 5 shows rain rate distributions for two years at Holmdel, N. J., measured on this rain gauge with integration time as a parameter. As expected, the distributions are functions of the integration time T .

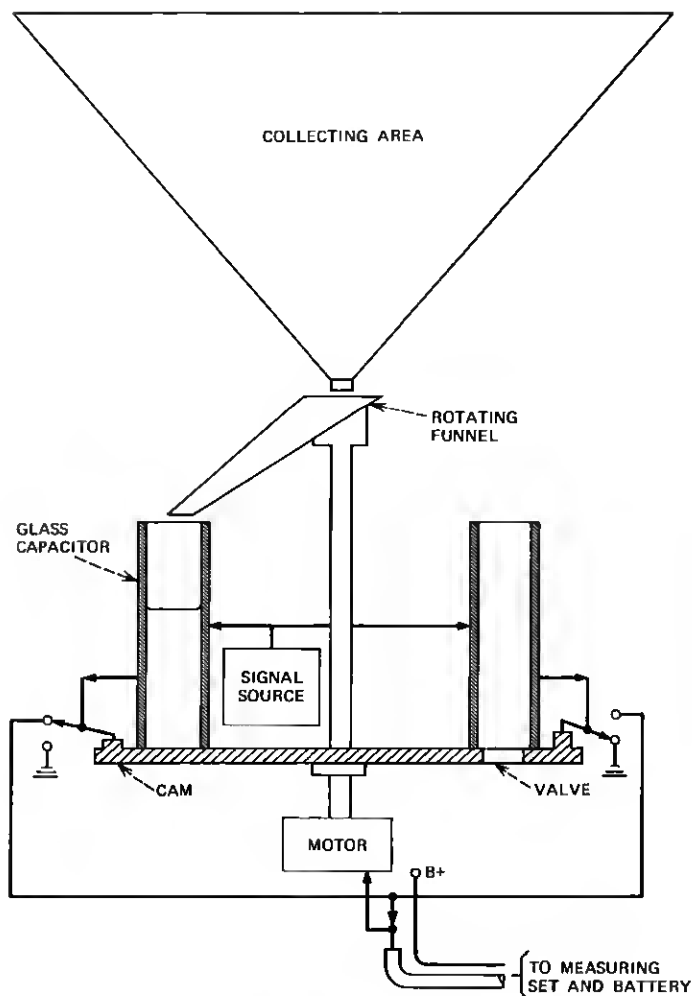


Fig. 3—The fast integrating rain gauge.

At present, only two of these fast rain gauges exist, so it has not been possible to obtain such distributions in many locations.

What is possible and practical is to measure distributions for an integration time of 1 minute from U. S. Weather Service rain gauge charts. We are therefore interested in converting 1-minute rain rate distributions to distributions at other measuring intervals. To facilitate this conversion, Fig. 6 has been prepared from Fig. 5. For many paths

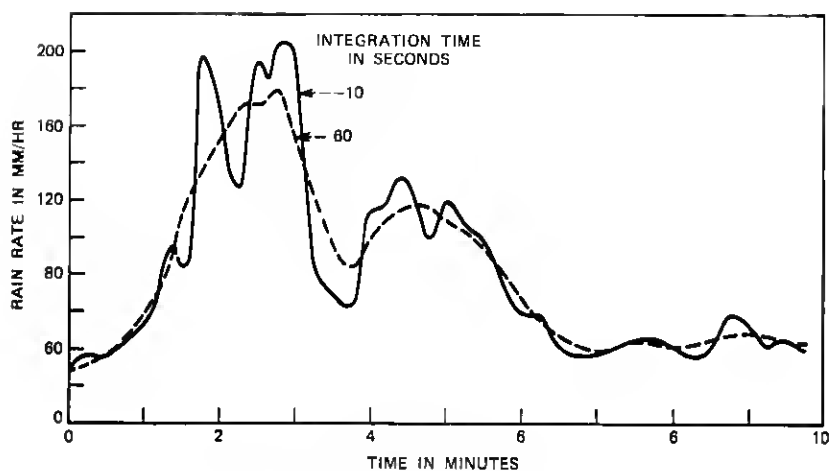


Fig. 4—Integrating rain gauge: storm of April 3, 1972.

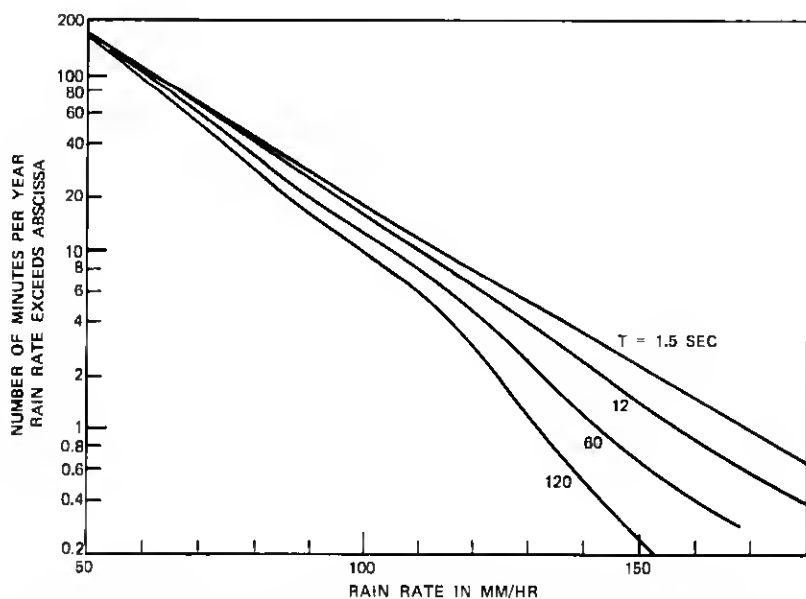


Fig. 5—Distribution of rain rates measured with fast-integrating rain gauge at Holmdel, N. J. for two years (1971 and 1972).

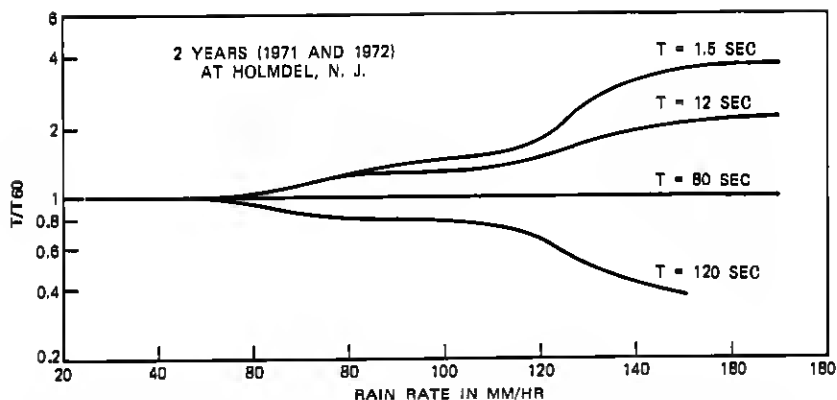


Fig. 6— T/T_{60} = (minutes per year rain rate exceeds abscissa for integration time T)/(minutes per year rain rate exceeds abscissa for 1-minute integration time).

of interest, the proper integration times fall between 12 and 120 seconds with the majority in the vicinity of 60 seconds. Thus, Fig. 6 shows that the distributions are not very sensitive to measuring interval out to rates of 120 millimeters per hour, which may correspond to a deep fade. Therefore, for many paths, 1-minute distributions will be adequate for design. For other paths, adjustments can be made from Fig. 6.

Note that the data shown in Fig. 6 are for a single location and cover a two-year period. It is not known to what extent these conversions apply to other locations, longer paths, and other periods of time.

V. THE EFFECTS OF NONSPHERICAL RAINDROPS

The theory was derived for spherical raindrops but, because raindrops are not quite spherical, the attenuation for vertical and horizontal polarizations are different. Morrison and Chu have computed the differential attenuation, the difference in attenuation between horizontally and vertically polarized waves, as a function of frequency for a specific raindrop model, and some of their results are shown in Fig. 7.⁸ The attenuation of a vertically polarized signal is less than that of a horizontally polarized signal, and we take the average of these to correspond to the attenuation caused by spherical raindrops.

The dashed lines in Fig. 7 are linear approximations to the data and may be used in the design of radio paths described in Section IX. As measured distributions of differential attenuation become available, it may be necessary to modify the results of Fig. 7.

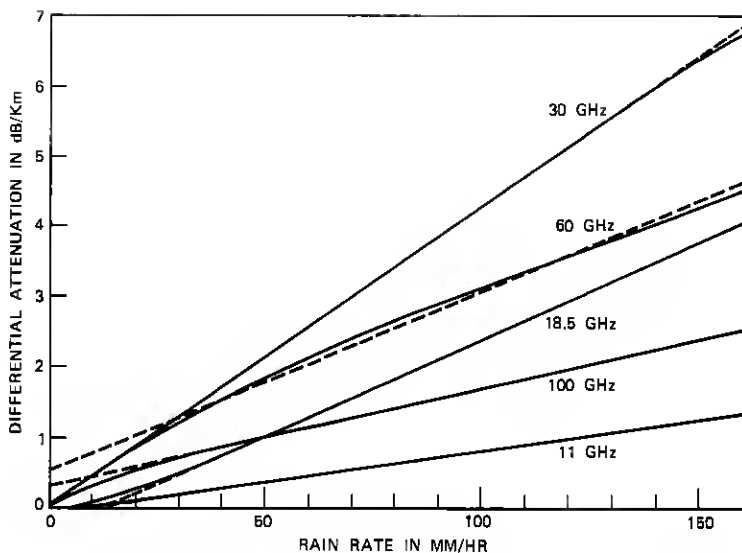


Fig. 7—Differential attenuation as a function of rain rate and frequency.

VI. COMPARISON OF THEORY AND EXPERIMENT USING DATA FROM THE FAST-INTEGRATING RAIN GAUGE

In this section and in Section VIII, comparisons are made between measured attenuation distributions and distributions predicted by the theory from measured rain rate distributions. Since the object of these comparisons is to test the efficiency of the procedure, it is important to use attenuation and rain rate distributions that are coincident in time and as near the same location as possible. In addition, distributions for time periods of less than one year were deemed inadequate.

The problem of estimating future attenuation distributions from existing rain rate distributions is different in that the time periods cannot be coincident. For this purpose, rain rate distributions covering a five-year interval are used in Section IX to illustrate the design of radio paths.

Two of the fast-integrating rain gauges are in service, one at Holmdel, N. J., and one at North Andover, Mass. At Holmdel, A. F. Dietrich and O. E. DeLange measured the attenuation on a 1.03-kilometer path at 60 GHz for the year 1971, and an attenuation distribution was obtained from these data. For the same year, estimated attenuation distributions for several rain gauge integration times were computed

from the fast-rain-gauge data. The distribution computed for an integration time of 12 seconds was the best fit to the measured attenuation distribution; the two distributions are shown in Fig. 8. Using a value of $T = 12$ seconds, the constant V_c in (1) was computed. Thus, based on this fit, we have an expression for rain rate integration time in seconds as a function of frequency and path length:

$$T \approx 1.05 \frac{\sqrt{\lambda L}}{\pi} \ln 32 \frac{L}{\lambda}. \quad (2)$$

At the Bell Laboratories facility in North Andover, Mass., G. H. Lentz measured attenuation on a 4.3-kilometer path at 18.5 GHz and rain rates with a fast-integrating rain gauge for three years.⁹ The appropriate rain rate integration time for this path is, from (2), about 45 seconds. By interpolation of Fig. 6, the 45-second and 60-second rain rate distributions are nearly identical, so the attenuation computed from a 1-minute distribution is accurate enough and is shown with the measured distribution of attenuation in Fig. 9.

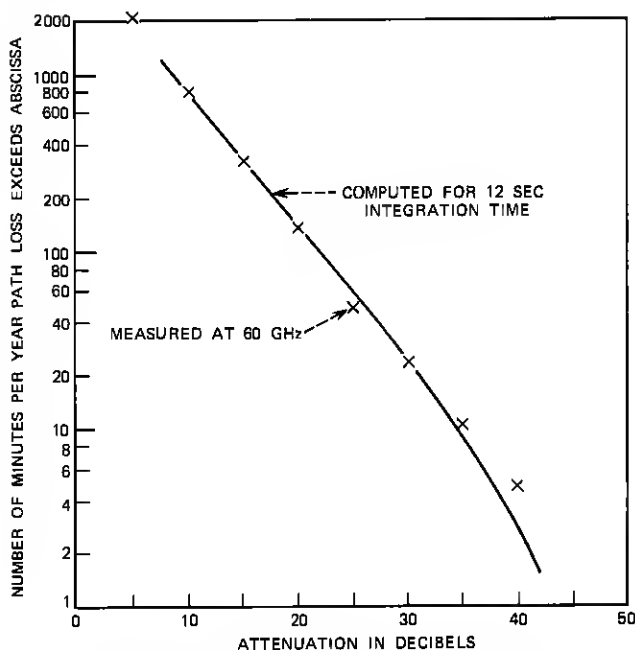


Fig. 8—Computed and measured attenuation distributions at 60 GHz for 1971.

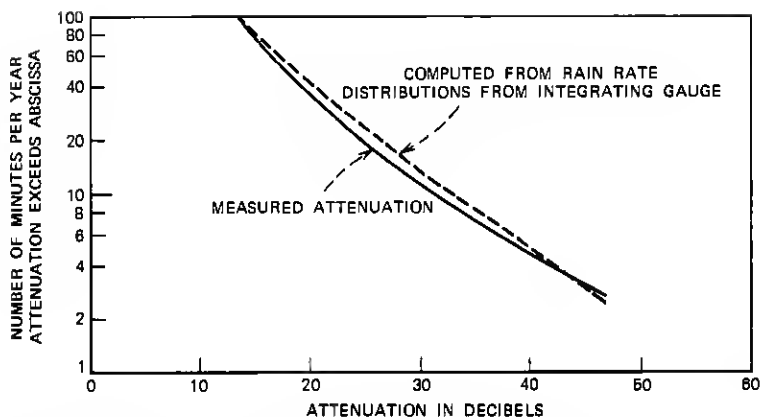


Fig. 9—Measured and computed attenuation distributions at North Andover, Mass., for three years (1971 to 1973), vertical polarization.

This is certainly satisfactory agreement between theory and experiment. The problem remains, however, of how to obtain suitable rain rate distributions for other locations.

VII. MEASUREMENT OF RAIN RATE DISTRIBUTIONS FROM U. S. WEATHER SERVICE DATA

The U. S. Weather Service operates rain gauges at many locations; for example, there are nearly 300 first-class weather stations, all of which operate rain gauges.⁴ There is, then, an immense amount of rain gauge data available which, if rain rates can be derived from it, can be used to produce accurate estimates of attenuation distributions anywhere in the country.

A weighing gauge measures the depth of water accumulated as a function of time, and a reproduction of part of such a record is shown in Fig. 10a. This chart does not show the rain rate, which is the derivative of the curve on the chart. However, a method has been devised for taking data at 1-minute intervals and using the data to compute the rain rate and its distribution.

Computing derivatives in this manner is notoriously inaccurate, and considerable processing is necessary to get accurate results, especially at high rain rates. The processing used in this work is described elsewhere.¹⁰ The rain rate computed from the chart in Fig. 10a is shown in Fig. 10b.

One-minute rain rate distributions for a 5-year period are shown in Fig. 12 for the locations indicated on the map of Fig. 11. The use of

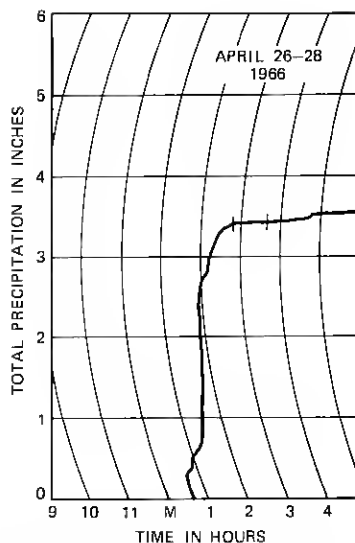


Fig. 10a—National Weather Service chart, Dallas, Texas.

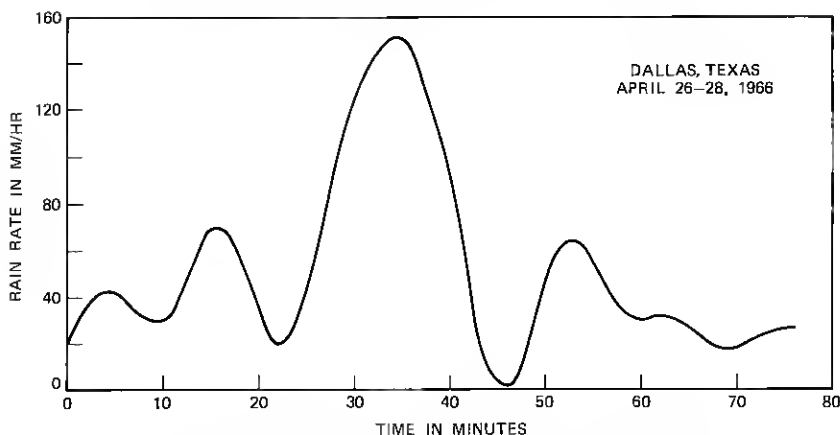


Fig. 10b—Rain rates vs time computed from weighing gauge data.

these distributions for the design of radio paths is demonstrated in Section IX.

VIII. COMPARISON OF THEORY AND EXPERIMENT USING U. S. WEATHER SERVICE DATA

Hudson, N. H., is about ten miles from the radio path at North Andover, Mass. The estimated attenuation distribution for the 4.3-kilometer path at 18.5 GHz was computed from the rain rate distribu-

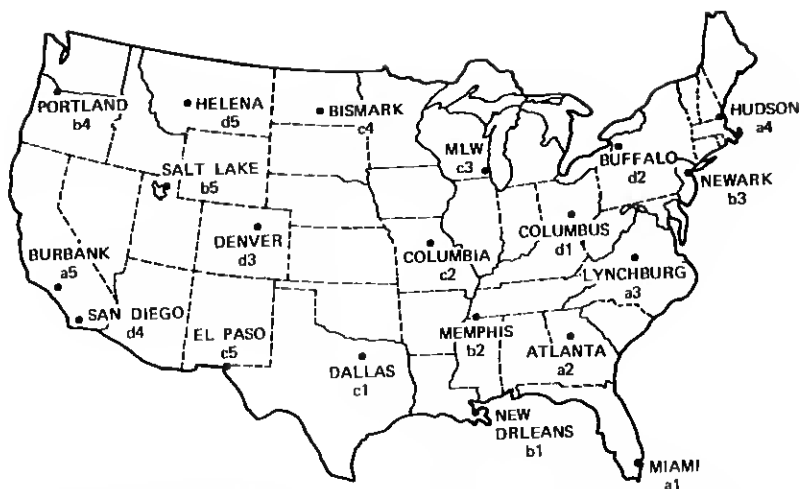


Fig. 11—Locations for which 1-minute rain rate distributions are shown in Fig. 12 (Key: d3 refers to Fig. 12d, curve 3).

tion measured at Hudson, N. H., as previously described. This result is shown with the measured distribution in Fig. 13.

Figure 14 compares a 3-year attenuation distribution, measured by R. A. Semplak on a 6.4-kilometer path at 18.5 GHz, to the estimated distribution computed from the Newark, N. J. rain rate distribution.¹¹ The distance from Newark to Crawford Hill, N. J., is about 30 miles.

Similarly, Fig. 15 compares the estimated attenuation distribution computed from the Atlanta, Ga., rain rate distribution with an attenuation distribution reported by S. H. Lin on a 5.15-kilometer path at 17.75 GHz near Palmetto, Ga., a distance of about 25 miles.¹²

It is evident from these comparisons that attenuation distributions can be estimated from rain rate distributions obtained by processing rain gauge charts. Design of radio paths using these distributions are now discussed.

IX. THE DESIGN OF SHORT RADIO PATHS

Determination of the path length for a specified outage time requires a knowledge of the wavelength and fading margin. Rain attenuation depends upon the wavelength, as already discussed in Section II. The fading margin requires a little more discussion. During periods of normal free-space propagation, the power received at the output port of the receiving antenna is given by

$$P_R = P_T \frac{A_T A_R}{\lambda^2 L^2}, \quad (3)$$

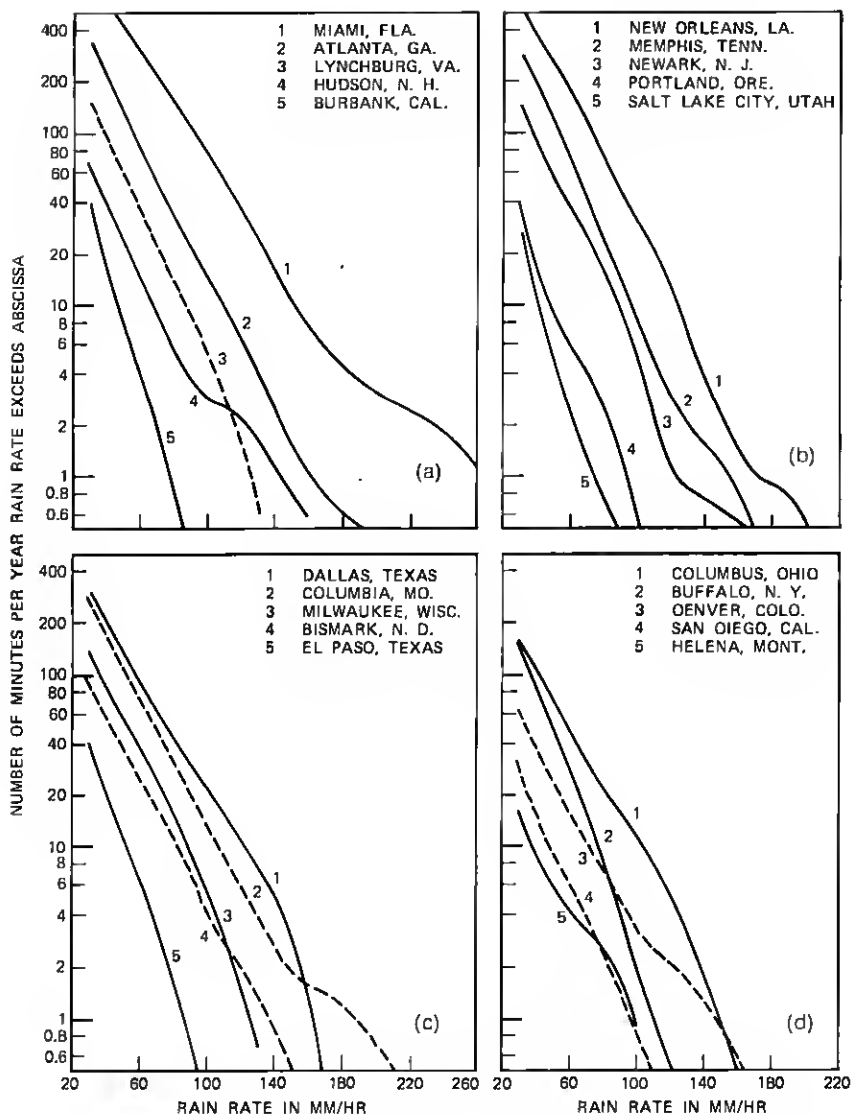


Fig. 12—Rain rate distributions average of five years (1966 to 1970).

where

P_T is the power at the input port of the transmitting antenna,
 P_R is the power received at the output port of the receiving antenna,

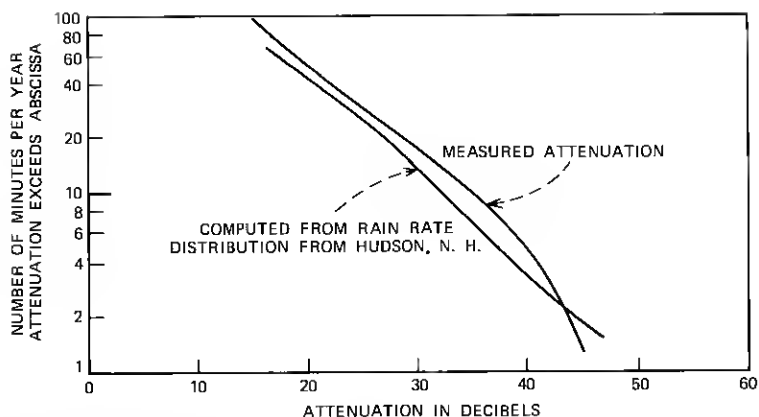


Fig. 13—Measured and computed attenuation distributions at North Andover, Mass., for year 1971, vertical polarization.

A_T , A_R are the effective areas of the transmitting and receiving antennas,

λ is the wavelength of the transmitted signal,

and

L is the distance between the transmitter and receiver.

The relationship between the effective antenna area and the gain, G ,

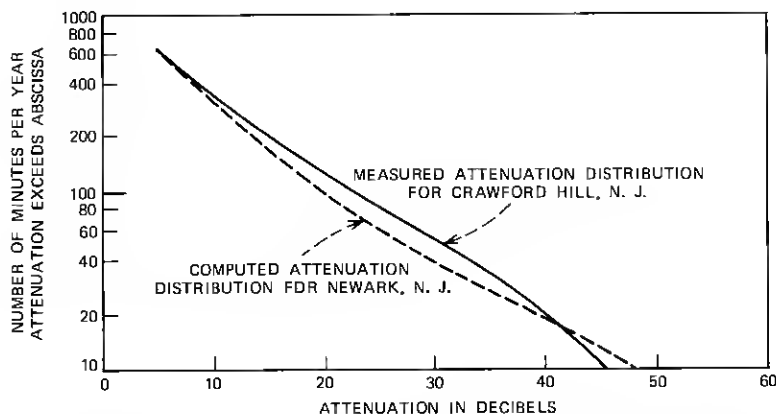


Fig. 14—Comparison of measured attenuation distributions at Crawford Hill, N. J., with computed attenuation distributions from rain rate data from Newark, N. J. for three years (1967 to 1969), vertical polarization.

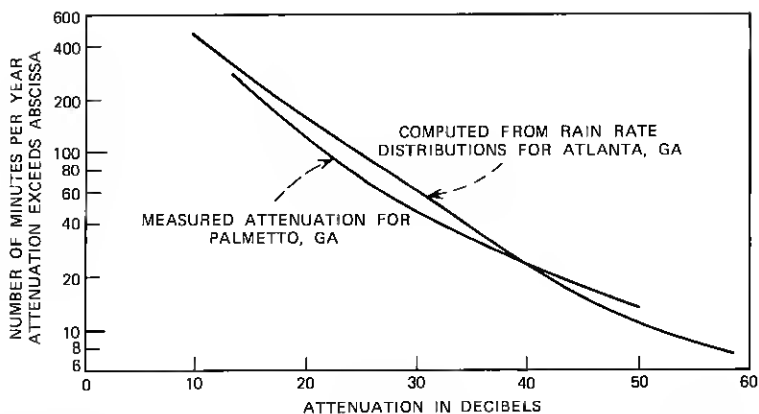


Fig. 15—Measured and computed attenuation distributions at Palmetto, Ga., for year 1971.

of the antenna is

$$G = \frac{4\pi A}{\lambda^2}.$$

In any system there is a minimum power, P_{\min} , that is required to meet the transmission objectives. If the received power falls below this value, the system is said to suffer an outage. The duration of the outage is the time interval during which the received power is less than P_{\min} , which depends upon the noise factor and bandwidth of the receiver and on the type of modulation and detection. With this convention, the fading margin in decibels is defined as

$$\alpha \equiv 10 \log P_R / P_{\min}. \quad (4)$$

Substituting for P_R from (3) reveals that the fading margin is a function of path length.

$$\alpha(L) = 10 \log \left(\frac{P_T}{P_{\min}} \times \frac{A_T A_R}{\lambda^2 L^2} \right). \quad (5)$$

It is convenient to write the fading margin for path length L in terms of the fading margin for a 1-kilometer spacing between antennas in decibels. Thus, if $\alpha(1)$ is the fading margin for a 1-kilometer path, the fading margin for an L -kilometer path in decibels is

$$\alpha(L) = \alpha(1) - 20 \log L. \quad (6)$$

From Fig. 1 we recall that the attenuation resulting from uniform rain as a function of rain rate can be described by linear functions over

the range of rain rates of interest. Thus, we have, from Fig. 1,

$$\gamma(L) = [aR + b]L, \quad (7a)$$

where

R is rain rate in millimeters per hour,

L is path length in kilometers,

and

a, b depend on wavelength.

The differential attenuation of Fig. 7 can be written

$$\delta\gamma(L) = (\delta a \times R + \delta b)L.$$

Using this expression, the attenuation of vertically and horizontally polarized signals can be written in the same form as (7a).

$$\gamma_v(L) = [(a - \delta a)R + (b - \delta b)]L, \quad (7b)$$

$$\gamma_h(L) = [(a + \delta a)R + (b + \delta b)]L. \quad (7c)$$

The parameters for several frequencies of interest are given in Table I.

When the rain attenuation exceeds the fading margin, the path is out of service. The rain rate for which the attenuation equals the fading margin can be found by setting $\alpha(L) = \gamma(L)$ in (6) and (7) to obtain

$$\alpha(1) = [aR + b]L + 20 \log L \quad (8a)$$

$$\alpha_v(1) = [(a - \delta a)R + (b - \delta b)]L + 20 \log L \quad (8b)$$

$$\alpha_h(1) = [(a + \delta a)R + (b + \delta b)]L + 20 \log L. \quad (8c)$$

These are nonlinear equations, and it is useful to present solutions in graph form, as in Fig. 16, for a frequency of 18.5 GHz.

Table I — Coefficients for attenuation as a function of rain rate

Frequency in GHz	a	b	δa	δb
11	0.045	-0.3	0.0046	-0.06
16	0.077	-0.08		
18.5	0.098	0	0.014	-0.2
30	0.178	1.5	0.0216	0
60	0.250	4.7	0.0129	0.25
100	0.287	5.1	0.0069	0.15
150	0.292	4.9		
300	0.275	4.45		

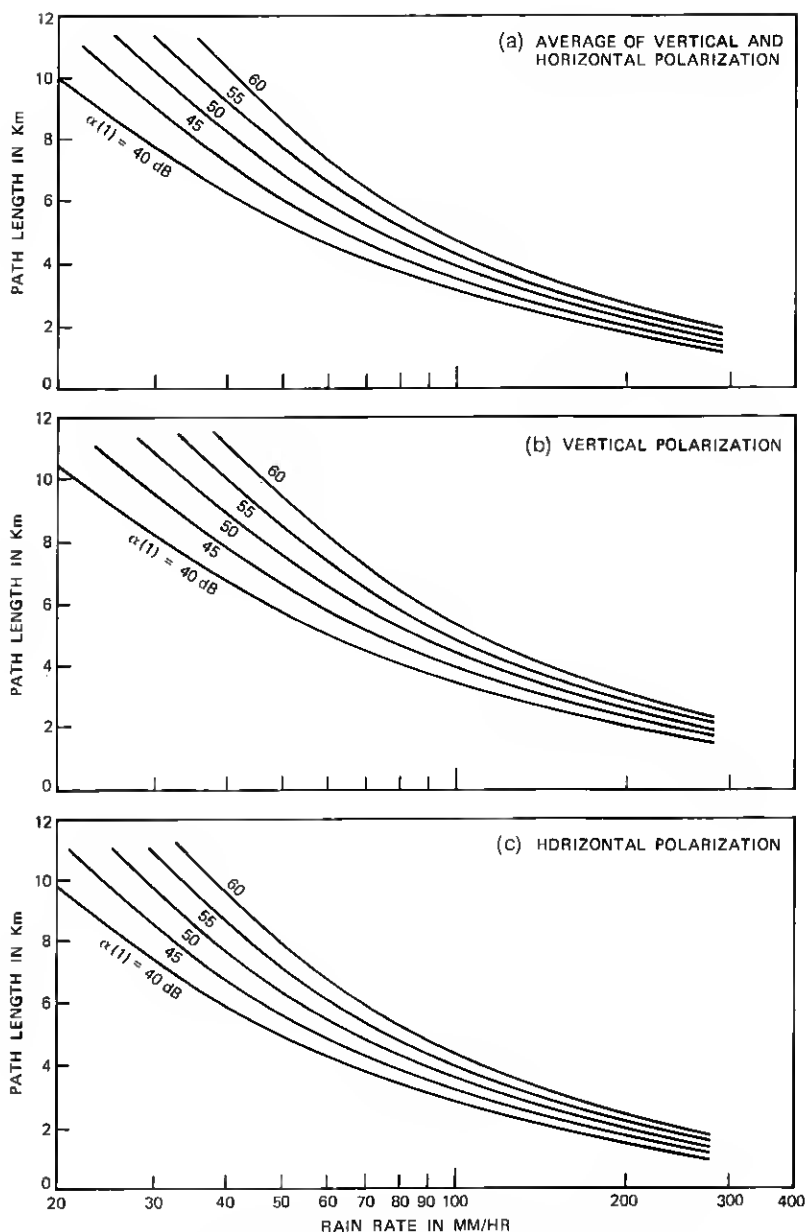


Fig. 16—Path length as a function of rain rate at 18.5 GHz.

We are now in a position to illustrate the design of short radio paths.

Example 1. Determine the outage time for a path of length $L = 6$ kilometers for a system characterized by a 1-kilometer fading margin, $\alpha(1) = 50$ dB, and an operating frequency of 18.5 GHz with vertical polarization. From (2), $T \approx 54$ seconds, so 1-minute rain rate distributions will suffice.

Enter Fig. 16b at $L = 6$ kilometers and $\alpha(1) = 50$ dB. The resulting rain rate is about 66 millimeters per hour. If the system is to be located in New Jersey, enter the rain rate distribution of Fig. 12h(3) at 66 millimeters per hour and note that the average outage time is about 28 minutes per year.

Example 2. A hypothetical 18.5-GHz system is to be built in New Hampshire between terminals separated by 40 kilometers. The service for which the system is intended requires that the average outage time not exceed 0.02 percent per year, which is 105 minutes. The system is characterized by a 1-kilometer fading margin of $\alpha(1) = 50$ dB.

We use the rain rate distribution for Hudson, N. H. Since there must be an integral number of hops in the system, we compute the total outage time for various numbers of hops, and the smallest number of hops resulting in an outage time of 105 minutes or less is the proper answer. We proceed as follows. For five hops, the path length would be 8 kilometers per hop. The polarization has not been specified, so Fig. 16a is used. From Fig. 16a, a rain rate of 41 millimeters per hour is obtained. Using this rain rate and the rain rate distribution for Hudson, N. H., an outage time of 35 minutes for an 8-kilometer path is found. There are five hops, so the total outage time is 175 minutes. It is clear that 8-kilometer paths are too long. Repeating the process for larger numbers of hops, it is instructive to plot the results, as in Fig. 17. From the figure we see that seven hops with average path length of 5.7 kilometers will be required. For paths of this length, $T \approx 52$ seconds, so again the 1-minute distribution will suffice.

It would be rare if the system could be laid out with equal path lengths. When the repeater sites are selected and the path lengths known, the expected system outage can be computed by summing the estimated outages for the individual paths as illustrated in the first example. The system outages computed in this manner will be conservative, since any joint path outages cannot be distinguished and, in effect, are counted as separate outages. To the extent that over-

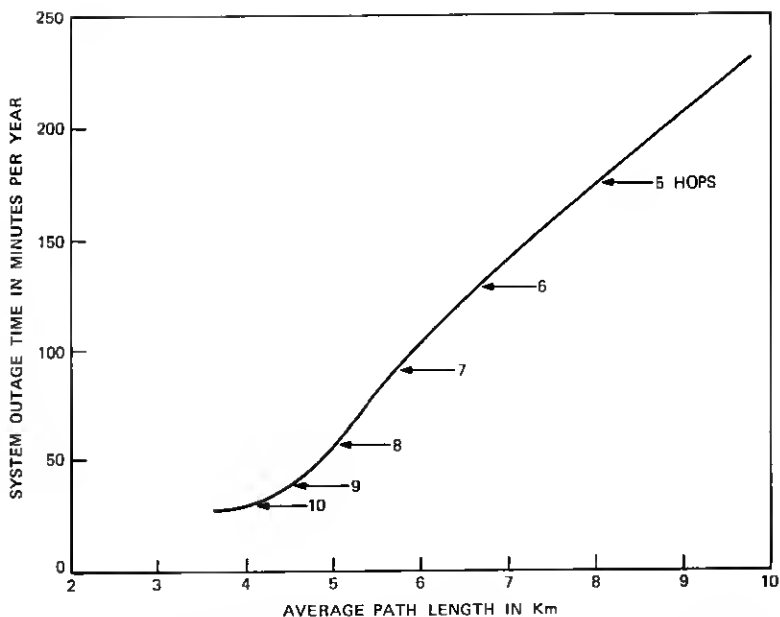


Fig. 17—System outage time, average path length, and number of hops for a total system length = 40 km and $\alpha(1) = 50$ dB.

lapping outages occur, the actual system outage time will be somewhat less than predicted.

X. CONCLUSION

A procedure has been described for designing short radio paths to meet transmission outage objectives when fading is caused by rain attenuation. The method is simple and examples are given. Data required include the operating frequency, the fading margin, the polarization to be used, and a suitable rain rate distribution. For many paths and frequencies of interest, accurate attenuation distributions can be estimated from 1-minute rain rate distributions. Examples of such distributions for a 5-year period, which were obtained by processing rain gauge data supplied by the U. S. Weather Service, have been presented. The design procedure is applicable to any section of the country for which suitable rain gauge data are available. This includes many of the several hundred stations operated by the U. S. Weather Service. Application of this method to longer paths is possible; work to accomplish this is presently under way.

XI. ACKNOWLEDGMENTS

We are indebted to F. M. Garland of the National Climatic Center for selecting the rain gauge charts used in this work. And we are grateful to Mrs. D. Vitello for writing and operating computer programs and Mrs. B. G. Griffin for assistance in the data processing.

REFERENCES

1. C. L. Ruthroff, T. L. Osborne, and W. F. Bodtmann, "Short Hop Radio System Experiment," *B.S.T.J.*, **48**, No. 6 (July-August 1969), pp. 1577-1604.
2. J. W. Ryde, "Echo Intensity and Attenuation due to Clouds, Rain, Hail, Sand, and Dust Storms at Centimeter Wavelengths," Rep. 7831, General Electric Company Research Laboratories, Wembley, England, October 1941. J. W. Ryde and D. Ryde, "Attenuation of Centimeter Waves by Rain, Hail, and Clouds," Rep. 8516, General Electric Company Research Laboratories, Wembley, England, August 1944. J. W. Ryde and D. Ryde, "Attenuation of Centimeter and Millimeter Waves by Rain, Hail, Fog, and Clouds," Rep. 8670, General Electric Company Research Laboratories, Wembley, England, May 1945.
3. C. L. Ruthroff, "Rain Attenuation and Radio Path Design," *B.S.T.J.*, **49**, No. 1 (January 1970), pp. 121-135.
4. A. H. Jennings, "Maximum Recorded United States Point Rainfall for 5 Minutes to 24 Hours at 296 First Order Stations," Technical Paper No. 2, U. S. Department of Commerce, Washington, D. C., Revised 1963.
5. R. G. Medhurst, "Rainfall Attenuation of Centimeter Waves: Comparison of Theory and Measurement," *IEEE Trans. Antennas and Propagation*, **AP-13**, No. 4 (July 1965), pp. 550-564.
6. D. E. Setzer, "Computed Transmission Through Rain at Microwave and Visible Frequencies," *B.S.T.J.*, **49**, No. 8 (October 1970), pp. 1873-1892.
7. W. F. Bodtmann, unpublished work, 1974.
8. J. A. Morrison and T. S. Chu, "Perturbation Calculations of Rain-Induced Differential Attenuation and Differential Phase Shift at Microwave Frequencies," *B.S.T.J.*, **52**, No. 10 (December 1973), pp. 1907-1913.
9. G. H. Lentz, unpublished work, 1974.
10. C. L. Ruthroff, "Computing Derivatives from Equally-Spaced Data," unpublished work.
11. R. A. Semplak, "The Influence of Heavy Rainfall on Attenuation at 18.5 GHz and 30.9 GHz," *IEEE Trans. Ant. and Prop.*, **AP-18**, No. 4 (July 1970), pp. 507-511.
12. S. H. Lin, unpublished work, 1972.

